Journal of Digital Imaging

Detecting Stripe Artifacts in Ultrasound Images

Adam Maciak,[1] Christian Kier,[2] Günter Seidel,[3] Karsten Meyer-Wiethe,[3] and Ulrich G. Hofmann[2]

Brain perfusion diseases such as acute ischemic stroke are detectable through computed tomography (CT)-/magnetic resonance imaging (MRI)-based methods. An alternative approach makes use of ultrasound imaging. In this low-cost bedside method, noise and artifacts degrade the imaging process. Especially stripe artifacts show a similar signal behavior compared to acute stroke or brain perfusion diseases. This document describes how stripe artifacts can be detected and eliminated in ultrasound images obtained through harmonic imaging (HI). On the basis of this new method, both proper identification of areas with critically reduced brain tissue perfusion and classification between brain perfusion defects and ultrasound stripe artifacts are made possible.

KEY WORDS: Ultrasound, stripe artifacts, moments, artifact segmentation, harmonic imaging, perfusion, stroke

INTRODUCTION

The successful treatment of cerebral vascular diseases is primarily based on the early and reliable detection of perfusion-reduced brain areas. Normally, brain perfusion is represented using various section diagram methods.

In clinical use, the magnetic resonance tomography has become a reliable method, especially because of its perfusion and diffusion imaging modes. Because of the low spatial resolution and the demanding technical prerequisites, perfusion computed tomography and single-photon emission computed tomography are becoming less relevant. A new diagnostic process for perfusion imaging of the human brain using ultrasound has been developed.[1,2] The diagnostic process is easy to use as a bedside method. It can be carried out repeatedly and provides reliable diagnoses, even for critical patients.[3–5]

The diagnostic imaging of the brain perfusion using ultrasound is mainly based on the application of ultrasound contrast agents (UCA) containing gas-filled micro-bubbles in a watery suspension. The properties of these micro-bubbles represent the main requirement for harmonic imaging (HI).[6–8] When the UCA is exposed to resonance oscillation, it emits harmonic waves of a stimulating ultrasound frequency. Using this method, a representation of the cerebral tissue can be obtained, which in turn can be used for the analysis of brain perfusion.[9–14]

Factors that reduce the quality of HI brain images are, for example, penetration depth, thickness of the cranial vault, blood flux speed, noise, and artifacts. Penetration depth can be increased by lowering the frequency at the expense of spatial resolution. A frequency of 1.8 MHz allows a penetration depth of approximately 10 cm, i.e., one brain hemisphere.[1,15]

Ultrasound imaging is heavily affected by noise. Especially speckle noise makes it necessary to employ noise reduction methods. Speckle noise occurs when sound waves interfere. At that moment, interfering waves can appear as a single signal with high amplitude. Several methods to

[1]*From the CADMEI GmbH, Otto-Hahn-Str. 6, 55424, Ingelheim, Germany.*

[2]*From the Institute for Signal Processing, University of Lübeck, Lübeck, Germany.*

[3]*From the Department of Neurology, University Hospital of Schleswig-Holstein, Kiel, Holstein, Germany.*

Correspondence to: Adam Maciak, tel: +49-6132-7135713; fax: +49-6132-713901; e-mail: am@avallia.com

doi: 10.1007/s10278-007-9049-0

reduce speckle noise have been developed. A fast and robust method is a nonlinear median filter.[15,16]

Another problem of ultrasound brain imaging is the appearance of stripe shadowing effects called stripe artifacts. The most common type of stripe artifacts is the border artifact that appears at the margin of the ultrasound cone. The most problematic stripe artifacts are the ones that pass through the ultrasound cone. It might happen that this artifacts shade perfusion-reduced brain tissue.[17,18] Figure 1 shows a parametric image of a particular brain area with two border artifacts and a thin stripe artifact that runs through the perfusion defect.

It is difficult to discriminate perfusion-reduced brain areas from artifact areas because both share similar features.[19,20] An automatic detection of stripe artifacts helps inexperienced physicians to distinguish between cerebral regions with reduced brain perfusion and artifacts, allowing a more definite statement about possible cerebral perfusion diseases.

Especially, the automatic detection of perfusion-reduced brain tissue fails if stripe artifacts are not entirely detected. This failure is mainly caused by the accumulated appearance of stripe artifacts. The correct and valid detection of stripe artifacts makes such automatic systems for computer-aided diagnosis possible.

HARMONIC IMAGING

There are two different principles of UCA application for the representation of brain perfusion. Bolus harmonic imaging (BHI) employs bolus injection; the other technique is based on continuous UCA supply.[17,21,22] In both methods, stripe artifacts occur.

The bolus method aims at detecting the bolus kinetic, i.e., the wash-in and wash-out process of UCA in the brain tissue. A BHI sequence consists of 20 to 40 images acquired at a frame rate of 2/3 Hz, showing the bolus kinetics of the UCA and reaching the brain tissue in about 10 s.[23] With increasing UCA concentration, the sensitivity of the perfused tissue increases rapidly to ultrasound signal, reaches its peak, and declines afterward (Fig 2).[24–26]

In the continuous supply method, a UCA steady state is reached in the brain tissue in which the diminution and replenishment kinetics can be examined. Diminution harmonic imaging (DHI) also makes use of the fact that ultrasound can destroy the gas-filled micro-bubbles of the contrast agent. By using high-intensity ultrasound pulses, micro-bubbles are destroyed. Bursting micro-bubbles emit ultrasound corresponding to the original concentration. The concentration curve combined with a UCA flow model permits calculation of the perfusion.[10,11,27]

Replenishment harmonic imaging (RHI) examines the duration of the refill process of the UCA in the brain tissue after destroying it. This method is very time-consuming, especially because measuring the concentration of the UCA destroys the micro-bubbles. A single measurement, thus, requires an intermediate steady state to avoid falsified sampling values of the time–intensity curve.[23]

A parameter commonly used in, e.g., BHI is the maximal intensity LPI($\overline{p}$) (LPI, local peak

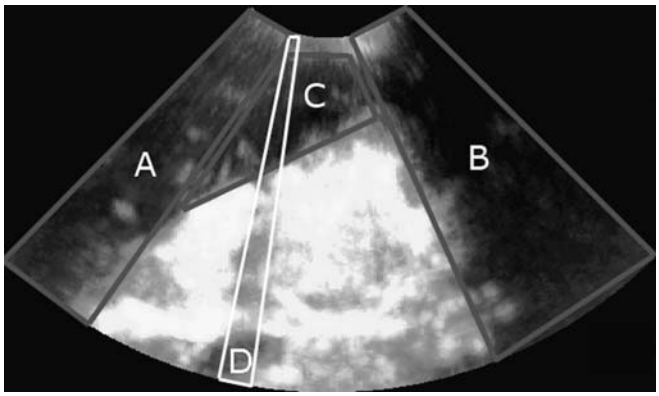

Fig 1. An example of a LPI parametric image of a brain area with one perfusion defect (*area C*) and two border stripe artifacts (*areas A and B*). A thin artifact runs through the perfusion defect (*area D*).

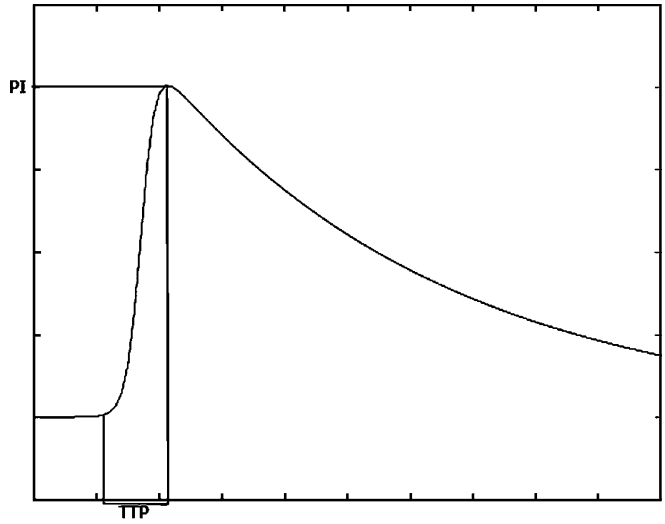

Fig 2. Time–intensity model curve with local peak intensity (*LPI*) and time to peak (*TTP*) parameters illustrated. The LPI value is the maximum of the signal intensity through time. The TTP value represents the amount of time from the beginning of contrast enhancement to the time reaching the peak.

intensity) at a pixel $(x, y) = \overline{p}$ from the image sequence. $\mathrm{TTP}(\overline{p})$ (TTP, time to peak) refers to the amount of time required to reach the maximal intensity.

The obtained values result in two parameter images (Fig. 3a and b), allowing identification of regions with reduced brain perfusion.[23,25,26] Both parameters are calculated for every pixel from all recorded images as follows:

$$\mathrm{TTP}(\overline{p}) = t_{\max}(\overline{p}) - t_0(\overline{p}) \quad (1)$$

$$\mathrm{LPI}(\overline{p}) = t_{\max}(\overline{p}) - i_0(\overline{p}) \quad (2)$$

With $t_0(\overline{p})$ referring to the time of the first significant intensity increase in the brain tissue as illustrated in Figure 1. Analyzing these two parameter images allows diagnoses of acute ischemic stroke.[25]

In areas of reduced perfusion, the signal intensity decreases and it takes longer until the respective peak intensity is reached. Multiple studies demonstrated the correlation between parameters LPI and TTP and reduced perfusion.[23,25,26] Further parameters can be extracted from the image sequences;[8,26] however, these do not seem to improve detection of perfusion-reduced

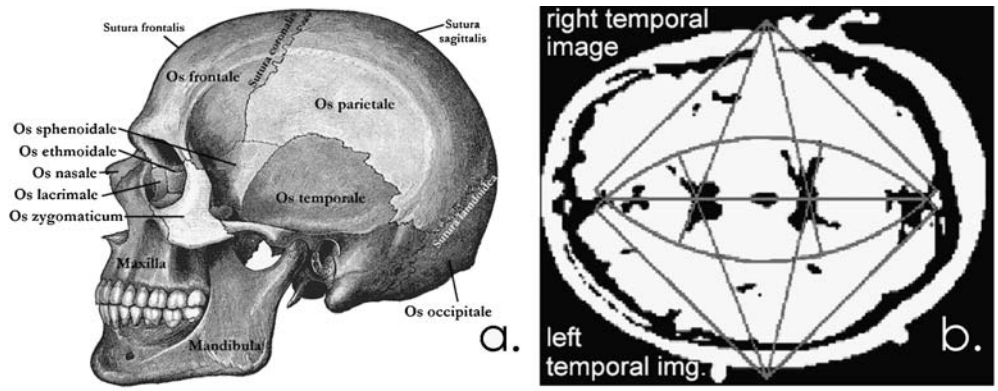

Fig 3. a Artifact origin: The cranial vault is formed by the frontal, parietal, and occipital bones. For an optimal signal echo, the ultrasound probe must be placed between vault and temporal bone. b The ultrasound scan between the cranial bones yields to a horizontal image of the brain tissue. The image quality is influenced by bone anomalies or by a too-small window of the bone segments.[23]

brain tissue.[26] In Kier et al.,[26] it was shown that a criterion for reduced perfusion is the reduction of the signal intensity to 33% of the maximal signal intensity. Another criterion is an increased TTP value. In Kier et al.,[26] 4 s are given as a significant TTP value. Requiring both criteria to be met in each pixel yields binary images giving an indication of reduced perfusion.

ARTIFACT DETECTION

To use ultrasound on cerebral tissue, the ultrasound probe has to be aligned between cranial vault and temporal bone so that the ultrasound beam passes through the thinnest part of the bones called temporal window (Fig. 3a and b). Bone segments and differences in thickness can obstruct and reflect ultrasound waves and, thus, prevent the ultrasound from reaching the brain tissue behind the cranial bones. This effect results in a striped diminution of the ultrasound cone along the direction of the beam propagation referred to as stripe artifacts (Fig. 1).

These stripe artifacts possess features characteristic of perfusion-reduced brain tissue: LPI is decreased, and significance of the TTP value is reduced. This makes it difficult to arrive at definite conclusions about perfusion in areas affected by stripe artifacts. However, if these areas are excluded, definite statements for the remaining areas are possible.

Stripe artifacts show a characteristic shape. Because of physical conditions, a stripe artifact extends along the complete cone of the ultrasound beam. If a stripe artifact is interrupted, it can only be caused by noise, vibrations, and other errors. Usually, stripe artifacts are rather slim. If the number of artifacts increases, the diagnostic relevance will decrease rapidly.

For the automated detection of stripe artifacts, our method proceeds by looks at the shape of the perfusion-reduced areas. If the area is line-shaped and aligned along the ultrasound cone, it is considered to be a stripe artifact.

Some stripe artifacts are not narrow. To detect such artifacts, which may also be fragmented by noise or other distortions, the ultrasound cone is divided into uniform sectors. Each sector is analyzed for stripe artifacts individually. Because these sectors are often narrow, a stripe artifact will mostly fill it only partially. Thus, a segmented stripe artifact must have a high eccentricity. A wide stripe artifact must have a high eccentricity in each of its sectors. The characteristic shape of a stripe artifact allows us to use eccentricity for identification, as it responds to line-shaped objects.

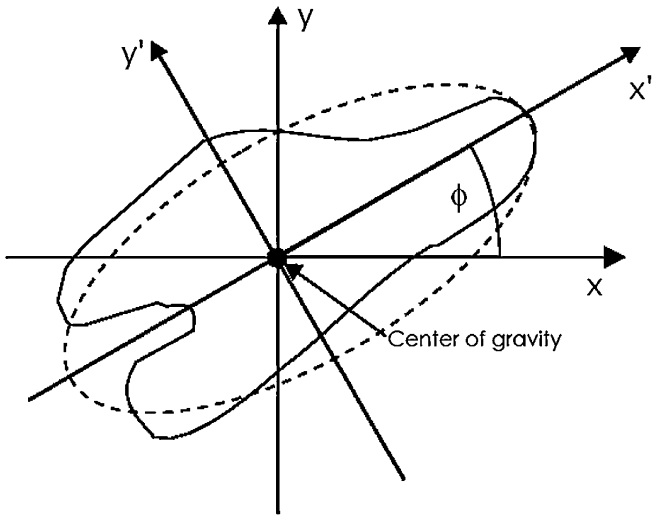

Fig 4. Ellipse with an irregular object. The fitting of an ellipse to an object results in the eccentricity [30]. High eccentricity values represent long and narrow objects. Low values represent circular objects.

Moments can represent the shape of an object and are defined for binary images as

$$\mu_{\mathrm{p,q}} = \sum_{p,q} (x_1 - \overline{x_1})^p (x_2 - \overline{x_2})^q \qquad (3)$$

with $\overline{x} = (x_1, x_2)$ as the center of gravity of the object.[28,29] The zero-grade moment $\mu_{0,0}$ is the total mass of the object. Eccentricity is calculated from the second-grade moments ($\mu_{0,2}$, $\mu_{2,0}$, $\mu_{1,1}$) as

$$\varepsilon = \frac{\left(\mu_{2,0} - \mu_{0,2}\right)^2 - 4\mu_{1,1}^2}{\left(\mu_{2,0} - \mu_{0,2}\right)^2} \qquad (4)$$

and returns a value between 0 for round and 1 for line-shaped objects.[31] Figure 4 shows how the eccentricity can be interpreted. It is a measure for an ellipse eccentricity that has been fitted to an irregular object.

For the detection of stripe artifacts, the images are preprocessed with a median filter of radius 5 to minimize effects of speckle noise. Then, the image sequence is examined applying rules 1 and 2 mentioned in "Harmonic Imaging," which results in two binary images LPI and TTP and gives the local peak intensity and time to peak for every pixel.

Let m be the maximum gray value in the LPI image. The image $\mathrm{BIN_{LPI}}$ results in comparing each pixel of LPI with $1/3m$ resulting in a binary value:

$$\mathrm{BIN_{LPI}}(\overline{p}) = \mathrm{LPI}(\overline{p}) < 0.33 \cdot m ? \mathrm{true} : \mathrm{false} \qquad (5)$$

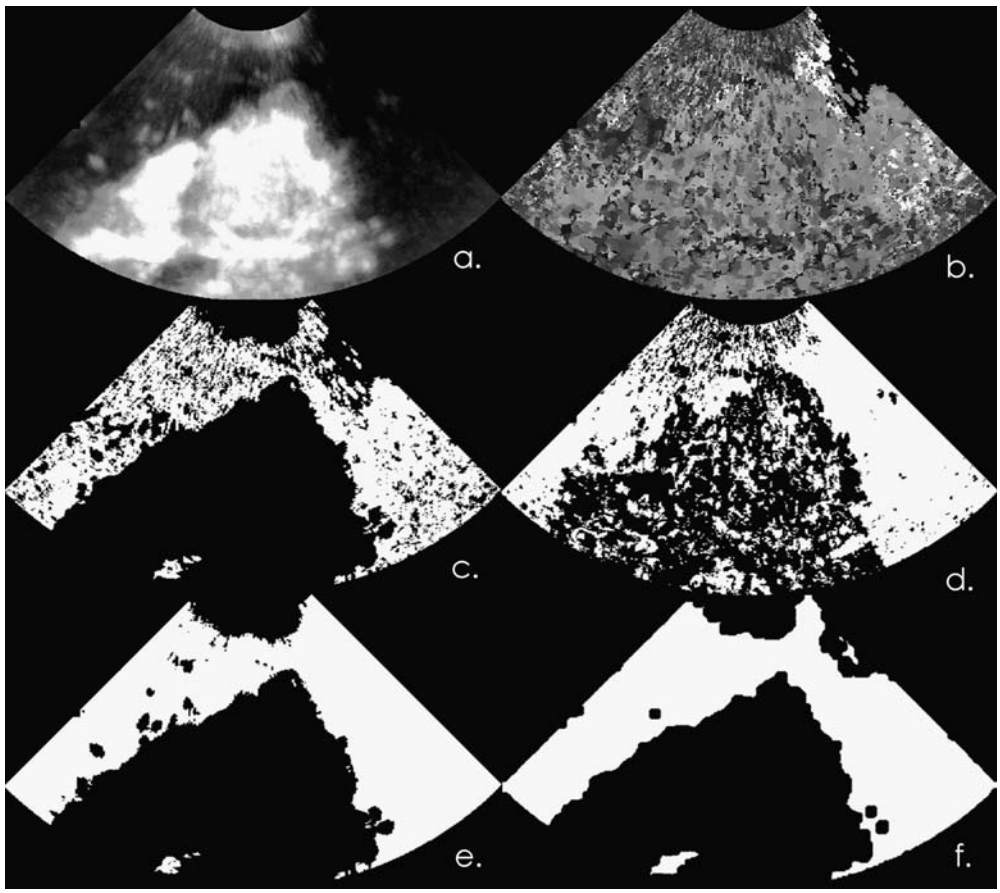

Fig 5. a The LPI image represents the maximum signal intensity for each pixel. The brighter the pixel, the higher is the signal intensity. b The TTP image represents the time until the peak in each pixel is reached. The brighter the pixel, the longer the time until the coordinate reaches the peak. c Binary peak intensity image after applying the 1/3-rule. *White pixels* represent coordinates that have a higher SI than 1/3 of the maximum SI in the whole image ($\mathrm{BIN_{LPI}}$). d Binary time to peak image after applying the 4 s-rule. *White pixels* represent coordinates ($\mathrm{BIN_{TTP}}$, e). Combined result of both binary images (result of AND-Operator). This image shows *white pixels* where the criteria of reduced perfusion apply ($\mathrm{BIN_{PERF}}$). f Result of application the morphological closing-operation with a circle structure element (diameter of 7).

Coordinates in the binary image $\mathrm{BIN_{LPI}}$ are set to 1 if the pixel is a candidate for perfusion-reduced tissue; otherwise, they are set to 0. Similar to the $\mathrm{BIN_{LPI}}$ image, a $\mathrm{BIN_{TTP}}$ image is generated. The image sequence is acquired with an interframe time of 1,500 ms. Thus, the TTP value has to be a least three frames to cover 4 s. Hence, the $\mathrm{BIN_{TTP}}$ image is 1 for each pixel if the TTP value is greater or equal to three frames, otherwise 0.

$$\mathrm{BIN_{TTP}}(\overline{p}) = \mathrm{TTP}(\overline{p}) \geq 4?\mathrm{true} : \mathrm{false} \qquad (6)$$

These two rules result in two binary images (examples in Fig. 5c and d). Next, both binary images will be combined pixelwise with the logical AND ($\oplus$) operator into one binary image $\mathrm{BIN_{PERF}}$:

$$\mathrm{BIN_{PERF}}(\overline{p}) = \mathrm{BIN_{TTP}}(\overline{p}) \oplus \mathrm{BIN_{LPI}}(\overline{p}) \qquad (7)$$

This resulting binary image may contain isolated white pixels (example in Fig. 5e). To remove these pixels and merge areas mostly filled with white pixels, a morphological closing operator with a circle structure element of radius 7 is applied (see example in Fig. 5f).

Next, the image is divided into 32 uniform sectors (Fig. 6a). The number of sectors has been proven experimentally and is a suitable trade-off between computing time and detection rate. Each sector contains n connected white objects that are segmented and labeled. Each object is then

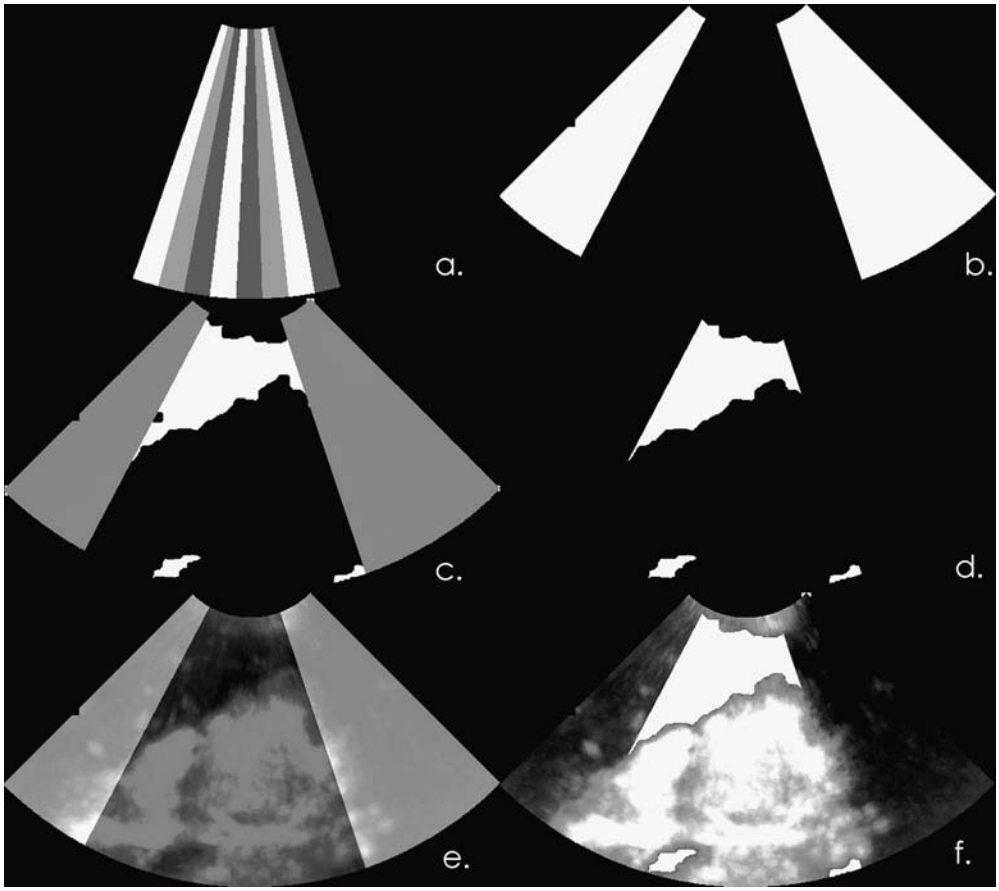

Fig 6. a The binary result image is divided into uniform sectors. This image shows a mask for such sectors. Each sector is tested for its eccentricity individually. b The result of the eccentricity tests. The image shows detected stripe artifacts. c Stripe artifacts (*gray*) displayed in the binary result image (*white*). d The stripe artifacts are removed by masking. The result of this is the perfusion defect. e Parametric image with superimposed stripe artifacts. f Perfusion defect superimposed in the parametric image. The *homogeneous white areas* represent perfusion defects.

analyzed for its eccentricity ε_i (Eq. 4). The eccentricity of the current sector can be computed by adding all eccentricities of the current sector to

$$E = \sum_{i=1} \varepsilon_i. \tag{8}$$

Next, the mass of each sector $M=\mu_{0,0}$ is determined (Eq. 3). S represents a constant denoting the mass of a complete white sector. If the ratio M/S is greater than 1/3 and $E/n>0.9$, this sector is considered to be a stripe artifact sector (Fig. 6b). The thresholds have been proven as being optimal in ROC analysis. This computation is done for each sector of the image. Following this, the BIN_{PERF} image is masked with the stripe artifacts image. After this step, only perfusion-reduced brain tissue will remain highlighted (Fig. 6c and d).

The workflow of the detection process is shown as an UML process in Figure 7.

RESULTS

For the validation of the proposed method, a study on BHI image sequences of 26 different patients has been conducted. The ethics committee approved of this study. All participants in the study gave their informed consent. The automatically detected artifact regions were compared to artifact regions marked by a clinical expert.

All 26 data sets showed stripe artifacts, 12 showed a perfusion deficit, and 10 were healthy. In four problematic cases, statement could be made concerning the perfusion because of bad image quality (US probe movement, insufficient bone window).

In these problematic cases, the true artifact regions were already very large. In 18 data sets, the stripe artifacts were detected correctly and precisely separated from perfusion deficits, leaving eight false detection results. Out of these false detection results, two were false negatives (one healthy, one diseased) because not all existing stripe artifacts had been detected. Out of the remaining six false positives, four were classified to be problematic cases because the detected regions were all even larger than the true artifacts because of bad image quality. In each of the two remaining data sets, one sector was classified as stripe artifact where a perfusion deficit almost

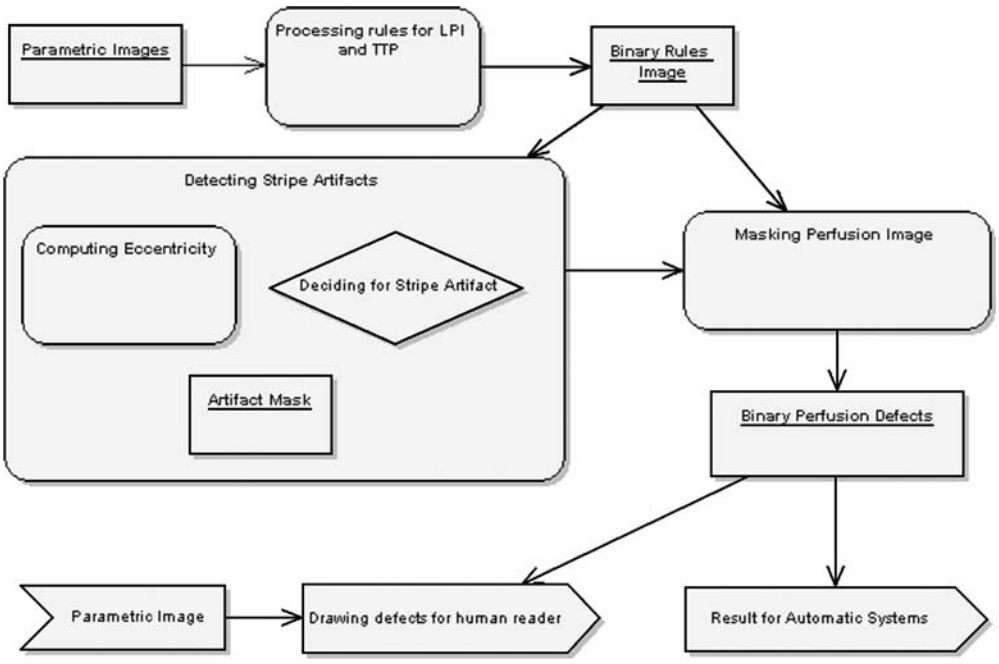

Fig 7. Process diagram of workflow: The binary image after combination of the rules is used to detect stripe artifacts. To do this, the image is divided in 32 uniform sectors. Each sector is tested individually for its eccentricity. The resulting mask is a combination of the eccentricity values of all sectors. After that, the resulting image can be taken for masking. The result is a binary mask with the perfusion-reduced brain tissue only.

extended over the complete depth of the ultrasound images. However, these sectors represented only 9 and 14% of the total perfusion defect respectively, so that 91 and 86% of the perfusion deficit, respectively, could still be classified correctly.

A good example of effectively detecting stripe artifacts is shown in Figures 5 and 6. Both stripe artifacts are detected correctly. The image in Figure 5e shows BIN_{PERF} to which the morphological operator is applied to reduce isolated pixels and merge areas resulting in the image in Figure 5f. Figure 6a to c shows the moment-based stripe artifacts detection process. Figure 6d shows the perfusion defect and Figure 6f the reduced tissue. Detected stripe artifacts are removed so that the resulting region corresponds to the perfusion defect (see Fig. 2, area C).

Figure 8 demonstrates problems that can occur with very large artifacts in one of the false negatives. The gap on the right in subfigures d and e belongs to the artifact. Because there is heavy noise in the image and every sector is tested separately, the fragment is too small to be classified as a stripe artifact.

CONCLUSIONS AND DISCUSSION

Our approach distinguishes stripe artifacts from perfusion defects, thus, allowing to eliminate stripe artifacts especially in transcranial ultrasonography. This method is a new step in gaining new information about perfusion-reduced brain tissue in image data acquired with HI. By detecting stripe artifacts correctly, it is possible

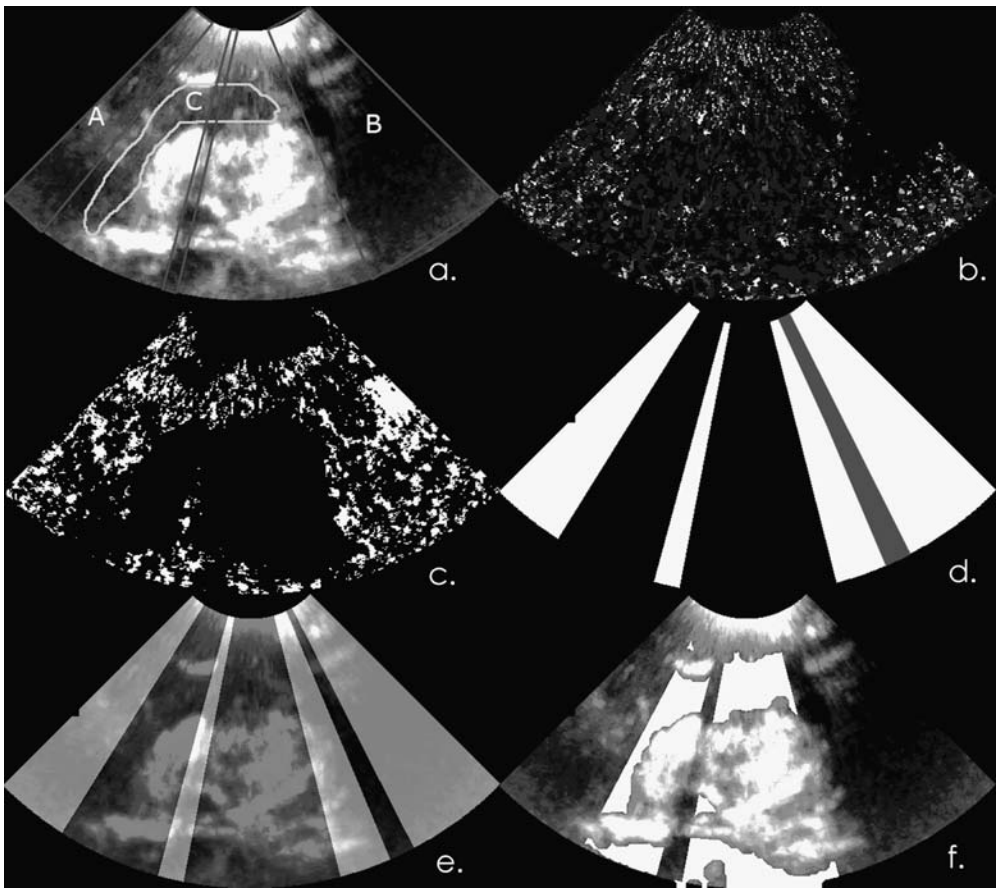

Fig 8. A false negative result: a LPI image with perfusion defect marked as C and two stripe artifacts labeled as in A and B. b TTP image. c Rule-based binary image (BIN_{PERF}). d Detected stripe artifacts. e The *gray* sector is not correctly classified as stripe artifact. Stripe artifacts displayed in LPI image. f Perfusion-reduced brain tissue (*white*) displayed in LPI image.

to differentiate stripe artifacts from perfusion defects automatically. This results in an expert system that especially aids inexperienced physicians in interpreting US images displaying cerebral perfusion. It provides a diagnosis quality similar to the one of expensive CT/MRI-based methods, but it offers the same advantages such as ultrasound imaging. It is cheap, less time-consuming and easy to use.

Problems of this method that have not been solved yet result in false negatives and false positives. The former occurs in wide stripe artifacts with intermittent noise or other anomalies resulting in single sectors that have not been detected as artifact. Context sensitive environment information could be used to overcome this problem. The latter occurs with images of bad quality or perfusion deficits expanding over the whole depth.

The first case is not an algorithmical problem, as even experts can make no decision. The latter usually only affects small parts of perfusion deficits and, thus, does not influence the diagnosis.

The presented method allows identifying stripe artifacts and distinguishing them from perfusion-reduced brain tissue. This makes the creation of an automatic system for detection of perfusion defects or stroke possible. To identify perfusion-reduced brain tissue, perfusion-reduced image regions are selected; stripe artifacts are detected and removed. The remaining image regions are perfusion-reduced brain areas without stripe artifacts.

ACKNOWLEDGMENT

The authors would like to thank Toni W. Vomweg and Sarah M. Hilbert, CADMEI GmbH, Germany, for their assistance and valuable input.

REFERENCES

1. Burns, PN: Harmonic imaging with ultrasound contrast agents. Clin Radiol 51:50, 1996

2. De Jong N, Frinking PJ, Bouakaz A: Detection procedures of ultrasound contrast agents. Ultrasonics 38:87–92, 2000

3. Harrer J: Second harmonic imaging of the human brain. Stroke 33(1):1530–1536, 2002

4. Liu Y: Cerebral hemodynamics in human acute ischemic stroke: a study with diffusion- and perfusion-weighted magnetic resonance imaging and SPECT. J Cereb Blood Flow Metab 20: 910–920, 2000

5. Meves S, Wilkening W, Thies T, Eyding J, Ermert HTP: Comparison between echo contrast agent-specific imaging modes and perfusion-weighted magnetic resonance imaging for assessment of brain perfusion. Stroke 33(1):2433–2437, 2002

6. Eyding J, Postert T, Wilkening W: Brain perfusion and ultrasonic imaging techniques. Eur J Ultrasound 16:91–104, 2002

7. Eyding J, Wilkening W, Reckhard M: Contrast burst depletion imaging—a new imaging procedure and analysis method for semiquantitative ultrasonic perfusion imaging. Stroke 34(1):77–83, 2002

8. Eyding J, Krogias C, Wilkening W: Parameters of cerebral perfusion in phase-inversion harmonic imaging (PIHI) ultrasound examinations. Ultrasound Med Biol 29(10): 1379–1385, 2003

9. Postert T, Muhs A, Meves SJF: Transient response harmonic imaging: an ultrasound technique related to brain perfusion. Stroke 29:1901–1907, 1998

10. Postert T, Hoppe P, Federlein JSH, Ermert H, Przuntek H, Büttner T, Wilkening W: Contrast agent specific imaging modes for the ultrasonic assessment of parenchymal cerebral echo contrast enhancement. Metabolism 20:1709–1716, 2000

11. Postert T, Hoppe P, Federlein J, Przuntek H, Büttner T, Helbeck S, Ermert H: Ultrasonic assessment of brain perfusion. Stroke 31:1460–1462, 2000

12. Seidel G, Kaps M, Greis C: Second harmonic imaging of a new ultrasound contrast agent (BY963): visualization of small cerebral arteries and analysis of regional cerebral blood flow. J Neuroimaging 7:230, 1997

13. Seidel G, Algermissen C, Kaps M: Harmonic imaging des Hirnparenchyms nach BR14 Bolusinjektion. Ultraschall in der Medizin 19:13, 1998

14. Wiesmann MGS: Ultrasound perfusion imaging of the human brain. Stroke 31:2421–2425, 2000

15. Nanda NCRS: Advances in Echo Imaging Using Contrast Enhancement, 1 edn. Norwell, MA: Kluwer, 1993

16. Noble JA: Ultrasound image segmentation: a survey. IEEE Trans Med Imag 25(8):987–1010, 2006

17. Seidel G, Algermissen C, Christoph A, Claassen L, Vidal-Langwasser MTK: Harmonic imaging of the human brain: visualization of brain perfusion with ultrasound. Stroke 31:151–154, 2000

18. Vollrath A, Kier C, Meyer-Wiethe K, Seidel G, Aach T: Detecting stripe artifacts in ultrasound parametric images. In: Biomedizinische Technik, volume 50. Berlin: Fachverlag Schiele und Schön, 2005, pp 1235–1236

19. Feigenbaum H: Echocardiography, 5th edn. Philadelphia: Lea and Febiger, 1994

20. Grolimund P: Transmission of ultrasound through the temporal bone. In Aaslid R Ed. Transcranial Doppler Sonography. Berlin Heidelberg New York: Springer, 1986

21. Wei K, Jayaweera AR Firoozan S, Linka A, Skyba DMSK: Quantification of myocardial blood flow with ultrasound-induced destruction of microbubbles administered as a constant venous infusion, volume 97. Berlin Heidelberg New York: Springer, 1998, pp 473–483

22. Seidel G, Algermissen C, Christoph A, Katzer T, Kaps M: Visualization of brain perfusion using harmonic grey scale and power doppler technology: an animal pilot study. Stroke 31:1728–1734, 2000

23. Metzler V, Seidel G, Meyer-Wiethe K, Wiesmann M, Aach T: Perfusion harmonic imaging of the human brain. In:

Ultrasonic Imaging and Signal Processing, volume 5035. Proceedings of SPIE, San Diego, CA, 2003, pp 337–348

24. Martina AD, Seidel G, Meyer-Wiethe KEA: Ultrasound contrast agents for brain perfusion imaging and ischemic stroke therapy—instrumentation in practice. J Neuroimaging 33(1): 1530–1537, 2005

25. Seidel GKMW: Harmonic imaging—Eine neue Methode zur sonographischen Darstellung der Hirnperfusion. Nervenarzt 72(1):600–610, 2001

26. Kier C, Toth D, Schindler LA, Meyer-Wiethe K, Cangür H, Seidel G, Aach T: Cerebral perfusion imaging with bolus harmonic imaging. In Walker WF, Emelianov SY Eds. Ultrasonic Imaging and Signal Processing, volume 5750. San Proceedings of SPIE, San Diego, CA, 2005, pp 437–446

27. Wilkening W, Postert T, Federlein J, Kono Y, Mattrey R, Ermert H: Ultrasonic assessment of perfusion conditions in the brain and in the liver. In: IEEE Ultrasonics Symposium, San Juan, Puerto Rico, 2000, pp 1545–1548

28. Teague MR: Image analysis via the general theory of moments. Optical Society of America, 1979, pp 920–930

29. Reiss TH: Recognizing planar objects, using invariant image features. In: Lecure Notes in Computer Science, volume 676. Berlin Heidelberg New York: Springer, 1993, p 30

30. Jähne, B.: Digital Image Processing, 6th edn. Berlin Heidelberg New York: Springer, 2005

31. Jain AK: Fundamentals of Digital Image Processing, 1st edn. Prentice-Hall, New Jersey, 1989